Electron-Beam-Induced Synthesis and Characterization of $W_{18}O_{49}$ Nanowires

Guozhen Shen,*,†,‡ Yoshio Bando,‡ Dmitri Golberg,‡ and Chongwu Zhou†

Department of Electrical Engineering, University of Southern California, Los Angeles, California 90089 and Nanoscale Materials Center, National Institute for Materials Science (NIMS), Namiki 1-1, Tsukuba, Ibaraki 305-0044, Japan

Received: January 2, 2008; In Final Form: January 23, 2008

Hierarchical core/shell $PbWO_4/WO_3$ microcrystals were subjected to convergent electron beam irradiation in a 300 kV transmission electron microscope, and $W_{18}O_{49}$ nanowires can be rapidly produced within 5 s irradiation. It was found that the produced $W_{18}O_{49}$ nanowires are single crystals with monoclinic structure. The lengths of these nanowires rapidly increase with the electron beam irradiation time and decrease with the increase of distance between source microcrystal and the formed nanowires. Our method is a quite simple and efficient way for the rapid synthesis of single-crystalline $W_{18}O_{49}$ nanowires and may be extended to synthesize other metal oxide nanowires with judicious choice of source materials.

1. Introduction

One-dimensional (1-D) metal oxide nanowires, such as ZnO, In_2O_3, SnO_2, WO_{3-x}, and MgO, etc., have attracted a lot of recent attention because of their unique properties for applications ranging from nanoelectronic devices, nanolasers, and solar cells to chemical and biosensors.[1−16] Among them, nanostructured tungsten oxide (WO_3) and its sub-oxides (WO_{3-x}, $x \geq 0$) are of particular interest due to their promising physical and chemical properties and their broad range of applications, such as in gas sensors, photocatalysts, electrochromic devices, field-emission devices, and solar-energy devices.[17−20] In particular, due to its unusual defect structure and promising properties in nanoscale regime, 1-D monoclinic $W_{18}O_{49}$ nanostructures have attracted much attention in recent years.[19−30] For example, single-crystal $W_{18}O_{49}$ nanowires have an turn-on field of 9.5 V/μm and can be used as potential field emitters.[27] $W_{18}O_{49}$ has sheet superconductivity which is closely related to its substructures and defects. Single-crystal $W_{18}O_{49}$ nanotips show good mechanical properties and can be laser welded and used as a point electron source.[29] Attracted by their important potential applications, much effort has been made to synthesize 1-D $W_{18}O_{49}$ nanostructures including nanowires, nanotubes, and nanobelts.[19−31] In most cases, 1-D $W_{18}O_{49}$ nanostructures were synthesized from high-temperature vapor or vapor−solid methods. For example, $W_{18}O_{49}$ microtrees consisting of numerous nanowires can be synthesized by heating a W foil at 1600 °C.[19] Nanoneedles of $W_{18}O_{49}$ can be obtained by reaction between W and water at 800−1000 °C.[25] Single-crystalline $W_{18}O_{49}$ nanowires were also synthesized by thermally evaporating WO_3 powders or thermally annealing W_2N films.[27,28] Low-temperature wet chemical methods were also developed recently to synthesize $W_{18}O_{49}$ nanowires. Monodispersed $W_{18}O_{49}$ nanorods with dimensional control in the quantum confinement regime were synthesized by hydrothermal reaction for 2−24 h.[31] $W_{18}O_{49}$ nanowires with a high aspect ratio were synthesized under hydrothermal conditions in the presence of surfactants.[24] Both high-temperature vapor methods and low-temperature solution methods obviously have their own advantages and disadvantages from different viewpoints. It is still challenging to develop a new synthetic method to synthesize $W_{18}O_{49}$ nanowires in a rapid and efficient way.

In this paper, we developed a rapid method for the synthesis of single-crystalline $W_{18}O_{49}$ nanowires by subjecting hierarchical core/shell $PbWO_4/WO_3$ microcrystals to convergent electron beam irradiation in a 300 kV transmission electron microscope. Using this method, single-crystalline $W_{18}O_{49}$ nanowires directly grown on the TEM grid not only can be synthesized within several seconds but also promise further single-nanowire properties measurements directly like field emission properties.

2. Experimental Section

Synthesis of Hierarchical Core/Shell $PbWO_4/WO_3$ Microcrystals. Single-crystal $W_{18}O_{49}$ nanowires grown on TEM grid were synthesized from hierarchical core/shell $PbWO_4/WO_3$ microcrystals, which were synthesized from a wet chemical method.[32] Briefly, $PbWO_4$ rod/dendrite-like crystals were first synthesized from the hydrothermal method using equivalent amounts of $Pb(AC)_2$ and Na_2WO_4 powders at 160 °C for 10 h. Then they were immersed in 4 M HNO_3 solution for 24 h. After being dried in air, the powders were subsequently calcined at 500 °C for 2 h.

Synthesis of $W_{18}O_{49}$ Nanowires. To get single-crystalline $W_{18}O_{49}$ nanowires, the hierarchical core/shell $PbWO_4/WO_3$ microcrystals were ultrasonically dispersed in ethanol and transferred to a carbon-coated TEM copper grid. Then the grid was inserted into a field emission JEM-3000F high-resolution transmission electron microscopy. In-situ irradiation nanowires-growth experiments were carried out with electron probes with a 5−100 nm diameter. A 300 keV accelerating voltage was applied through all experiments.

Characterization. The structures and compositions of the obtained products were characterized using a field emission JEM-3000F high-resolution transmission electron microscopy equipped with X-ray dispersive energy spectrometer and an Akashi 002B transmission electron microscope.

3. Results and Discussion

Figure 1a shows the SEM image of the hierarchical core/shell $PbWO_4/WO_3$ microcrystal precursors, which consist of

* To whom correspondence should be addressed. E-mail: guozhens@usc.edu; gzshen@ustc.edu.
† University of Southern California.
‡ National Institute for Materials Science.

10.1021/jp8000338 CCC: $40.75
Published on Web 03/20/2008

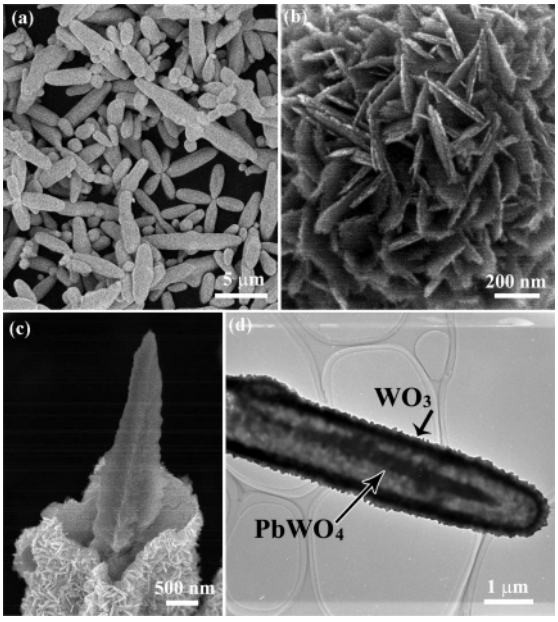

Figure 1. (a) Low-magnification SEM image of the hierarchical core/shell $WO_3/PbWO_4$ microcrystals. (b) High-magnification SEM image taken from a $WO_3/PbWO_4$ microcrystal, indicating the hierarchical structure. (c) SEM image of a broken microcrystal clearly showing core/shell structure. (d) TEM image of a core/shell $WO_3/PbWO_4$ microcrystal.

numerous microrods and dendrites. The lengths of these precursor crystals range from 1 to about 10 μm. Interestingly, the high-magnification SEM image shown in Figure 1b reveals that all of them are not with smooth surfaces but have a rough hierarchical surface. In other words, the surfaces of these precursors are composed of many tiny nanoplatelets standing perpendicular to the surfaces. Typical nanoplatelets are of uniform thickness of tens of nanometers. Characterization by X-ray diffraction (XRD) reveals that the as-synthesized precursors consist of two typical phases, the monoclinic WO_3 and tetragonal $PbWO_4$, confirming formation of hierarchical core/shell $PbWO_4/WO_3$ microcrystal precursors. The core/shell structures were well verified from a SEM image of a broken crystal as depicted in Figure 1c. X-ray energy-dispersive spectra (EDS) taken from this crystal reveal that the inner part is $PbWO_4$ while the outer shells are WO_3, also confirming formation of hierarchical core/shell $PbWO_4/WO_3$ microcrystal precursors. A TEM image of a core/shell $PbWO_4/WO_{34}$ microrod is shown in Figure 1d. The clear contrast variation between the core and the shell provides more evidence for the core/shell structures.

These hierarchical core/shell $PbWO_4/WO_3$ microrods/dendrites are sensitive to an electron beam (EB) under TEM observations. Figure 2a and b shows TEM images of a core/shell $PbWO_4/WO_3$ microrod after irradiated under EB for 10 and 30 s, respectively. From these images two phenomena are clearly observed. One is that the core/shell structure is a little damaged with the increase of irradiation time. Another is that nanowires are continuously produced around the precursor after irradiation. The length and density of the produced nanowires gradually increase as indicated by arrows in these images. The observations indicate that these core/shell microcrystals can be used as efficient precursors for the synthesis of nanowires.

Figure 3a−c shows typical TEM images with different magnifications of the nanowires after EB irradiated for 30 s. It is obvious that nanowires are produced efficiently on the TEM grid. All nanowires have uniform diameters of about 10 nm and lengths of about 100 nm with smooth surfaces. The EDS

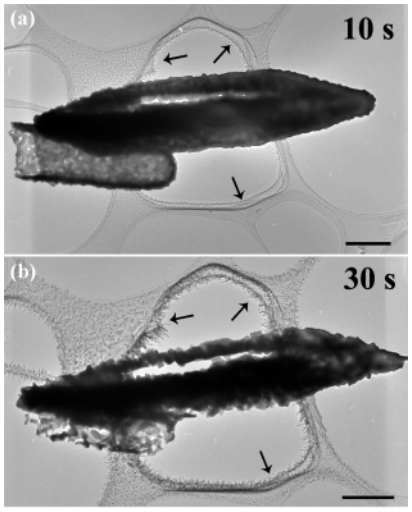

Figure 2. TEM images of a core/shell $WO_3/PbWO_4$ microcrystal after electron beam irradiation for different times: (a) 10 and (b) 30 s. Scale bars are 500 nm.

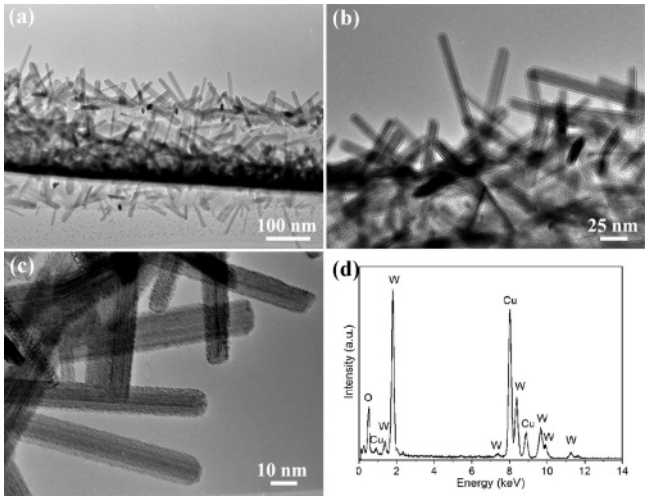

Figure 3. (a−c) TEM images with different magnifications of the produced $W_{18}O_{49}$ nanowires. (d) Nanobeam EDX spectrum taken from a single $W_{18}O_{49}$ nanowire.

spectrum of the nanowires shown in Figure 3d shows that they are composed of W and O with an approximate atomic ratio close to $WO_{2.72}$, indicating that these nanowires are $W_{18}O_{49}$ nanowires. In this spectrum, the signals of Cu come from the TEM grid.

Detailed structural analysis of the products was further carried out using high-resolution TEM (HRTEM). Figure 4a and b shows HRTEM images taken from two $W_{18}O_{49}$ nanowires. Shown in Figure 4c and d is the fast Fourier transform (FFT) pattern and selected area electron diffraction (SAED) pattern taken from the nanowires. Both show obvious streaking around diffraction spots, revealing the existence of stacking faults formed in the direction normal to the [010] direction. Such planar defects are commonly observed in many kinds of 1-D nanostructures, such as SiC nanowires, WO_3 nanowires, etc.[33−36] A lattice-resolved HRTEM image of the $W_{18}O_{49}$ nanowire is shown in Figure 4e. The clearly observed spacing of the lattice fringes was about 0.38 and 0.37 nm, corresponding to the [010] and [103] planes of a monoclinic $W_{18}O_{49}$, respectively. This result is in good agreement with the FFT and SAED results. All of the above discussions indicate that single-crystalline monoclinic $W_{18}O_{49}$ nanowires are synthesized in the present work with preferred growth direction along the [010] orientation.

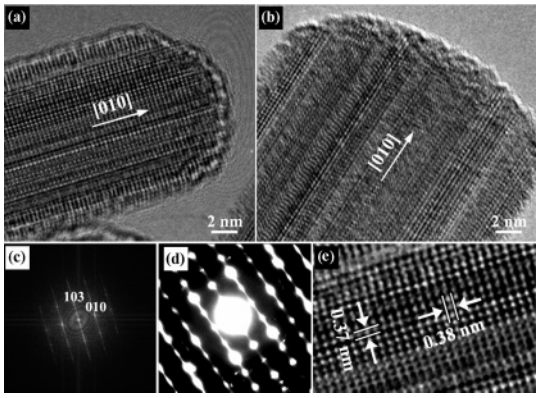

Figure 4. (a, b) Lattice-resolved HRTEM images of two $W_{18}O_{49}$ nanowires. (c) FFT pattern and (d) SAED pattern of the $W_{18}O_{49}$ nanowires. (e) Higher magnification HRTEM image clearly showing the lattice distance of about 0.38 and 0.37 nm corresponding to the (010) and (103) planes of monoclinic $W_{18}O_{49}$.

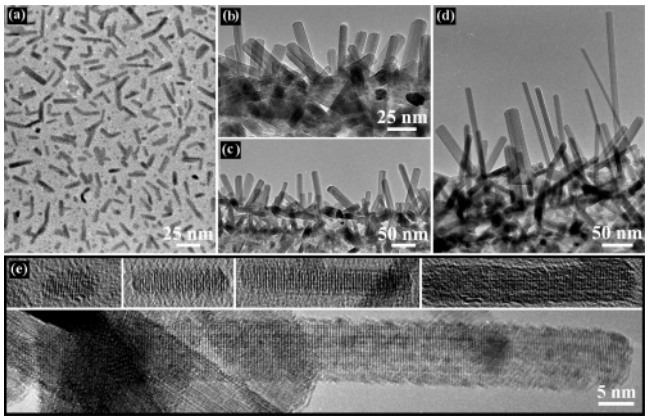

Figure 5. (a−d) TEM images of the produced $W_{18}O_{49}$ nanowires after different EB irradiations. (e) HRTEM images of $W_{18}O_{49}$ nanowires with different lengths.

It is well known that during TEM observations when a high-energy electron passes through a specimen its energy may partially be transferred to the target and enhance the movement of atoms. If the electron beam intensity goes above the threshold, damage to the target is usually caused.[37] The beam damage is generally dominated by direct displacement of atoms from a specimen, namely, knock-on displacement. This damage can occur within a very short time of around 10 ps to produce atomic defects. In the present work, when high-energy EB passed through hierarchical core/shell $PbWO_4/WO_3$ microcrystals, the core $PbWO_4$ species decompose and generate $W_{18}O_{49}$ instead of WO_3 due to the lack of enough oxygen in high-vacuum microscopy. In the experiments the wrapped WO_3 shell is quite stable, and they prevent the abrupt consuming of inner $PbWO_4$ species, thus resulting in slow release of newly generated $W_{18}O_{49}$, which deposited on the copper grid to form $W_{18}O_{49}$ as seeds for further nanowire growth. If irradiated for enough time, 1-D $W_{18}O_{49}$ nanowires are obtained. In fact, if only $PbWO_4$ microcrystals were used as the precursors instead of the core/shell $PbWO_4/WO_3$ microcrystals, only $W_{18}O_{49}$ particles with large size distributions are obtained instead of nanowires. Whereas if only WO_3 shells were used in the experiments, no $W_{18}O_{49}$ species were generated since they are relatively stable to an electron beam.

We found that the length and density of the produced $W_{18}O_{49}$ nanowires gradually increased with the increase of EB irradiation time. Figure 5 shows TEM images of $W_{18}O_{49}$ nanowires produced after EB irradiated for 5, 15, 30, and 50 s. It can be seen that small $W_{18}O_{49}$ nanowires can be produced within 5 s, which have lengths of about 20 nm (Figure 5a). When irradiated for 15 s, most of the lengths of the produced $W_{18}O_{49}$ nanowires increased to about 35 nm (Figure 5b). With a further increase of EB irradiation, the lengths of the produced nanowires further increased from 35 nm after 15 s irradiation (Figure 5b) and 80 nm after 30 s irradiation (Figure 5c) to several hundred nanometers after 50 s irradiation (Figure 5d). It is expected that the diameters of $W_{18}O_{49}$ nanowires will gradually increase until all the precursors are exhausted. Figure 5e shows some HRTEM images of the synthesized $W_{18}O_{49}$ nanowires with different lengths collected after electron beam irradiation time. It can be seen that all the nanowires are of single-crystalline nature and with the preferred growth direction along the [010] orientation.

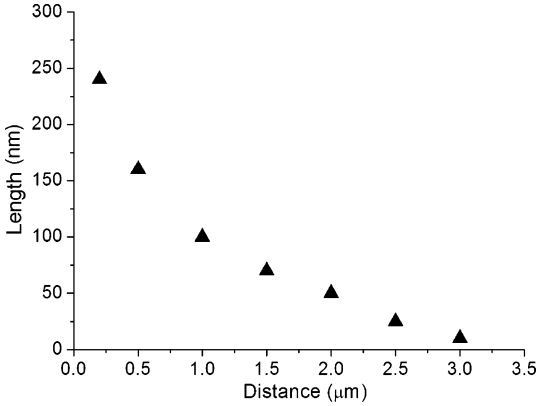

Figure 6. WO_3 nanowires length versus distance between source microcrystal and the formed $W_{18}O_{49}$ nanowires.

Besides EB irradiation time, the distance between the precursor and the target $W_{18}O_{49}$ nanowires also influences the lengths of the formed $W_{18}O_{49}$ nanowires. It is known that, under electron beam irradiation, if the irradiated precursor is viewed as the point source, the source flux will decrease with the increase of the distance between the source and the target position. Figure 6summarizes the relationship between the lengths of $W_{18}O_{49}$ nanowires and the distance between the precursor and the target $W_{18}O_{49}$ nanowires after being EB irradiated for 50 s. The plot shows that $W_{18}O_{49}$ nanowires have average lengths decreasing from ca. 250, 160, 70, 45, and 25 to 10 nm with the increase of distances from 0.2, 0.5, 1.0, 1.5, 2.0, and 2.5 μm to 3.0 μm, clearly verifying that the lengths of $W_{18}O_{49}$ nanowires continuously decrease with the increase of deposition distance.

4. Conclusion

We report the rapid synthesis of $W_{18}O_{49}$ nanowires. Subjecting hierarchical core/shell $PbWO_4/WO_3$ microcrystal precursors to convergent electron beam irradiation in a 300 kV transmission electron microscope, $W_{18}O_{49}$ nanowires can be rapidly produced within 5 s irradiation. Both EB irradiation time and distance between the precursor and the produced nanowires have an influence on the lengths of the final $W_{18}O_{49}$ nanowires. The present method not only provides a simple and rapid method for the efficient synthesis of single-crystalline $W_{18}O_{49}$ nanowires but also makes it possible to directly manipulate a single such synthesized $W_{18}O_{49}$ nanowire precisely and measure the properties of a single $W_{18}O_{49}$ nanowire, such as field emission properties, mechanical properties, etc.

Acknowledgment. We thank Dr. Chen at the National Institute for Materials Science for providing the precursors and

the Center for Electron Microscopy and Microanalysis (CEMMA, USC) for use of their facilities.

References and Notes

(1) Pan, Z. W.; Dai, Z. R.; Wang, Z. L. *Science* **2001**, *291*, 1947.
(2) Dai, Z. R.; Pan, Z. W.; Wang, Z. L. *Adv. Funct. Mater.* **2003**, *13*, 9.
(3) Wang, Z. L.; Song, J. H. *Science* **2006**, *312*, 242.
(4) Kuang, Q.; Lao, C. S.; Wang, Z. L.; Xie, Z. X.; Zheng, L. S. *J. Am. Chem. Soc.* **2007**, *129*, 6070.
(5) Ju, S.; Facchetti, A.; Xuan, Y.; Liu, J.; Ishikawa, F.; Ye, P.; Zhou, C. W.; Marks, T. J.; Janes, D. B. *Nat. Nanotechnol.* **2007**, *2*, 378.
(6) Liu, Z.; Zhang, D.; Han, S.; Li, C.; Tang, T.; Jin, W.; Liu, X.; Lei, B.; Zhou, C. W. *Adv. Mater.* **2003**, *15*, 1754.
(7) Li, C.; Zhang, D.; Liu, X.; Han, S.; Tang, T.; Han, J.; Zhou, C. W. *Appl. Phys. Lett.* **2003**, *82*, 1613.
(8) Liu, B.; Zeng, H. C. *J. Am. Chem. Soc.* **2004**, *126*, 16744.
(9) Liu, B.; Zeng, H. C. *Chem. Mater.* **2007**, *19*, 5824.
(10) Wang, Y.; Zeng, H. C.; Lee, J. Y. *Adv. Mater.* **2006**, *18*, 645.
(11) Shen, G. Z.; Bando, Y.; Liu, B. D.; Golberg, D.; Lee, C. J. *Adv. Funct. Mater.* **2006**, *16*, 410.
(12) Shen, G. Z.; Bando, Y.; Lee, C. J. *J. Phys. Chem. B* **2005**, *109*, 10779.
(13) Kar, S.; Pal, B. N.; Chaudhuri, S.; Chakravorty, D. *J. Phys. Chem. B* **2006**, *110*, 4605.
(14) Kar, S.; Dev. A.; Chaudhuri, S. *J. Phys. Chem. B* **2006**, *110*, 17848.
(15) Li, Y. B.; Bando, Y.; Golberg, D.; Liu, Z. W. *Appl. Phys. Lett.* **2003**, *83*, 999.
(16) Zhan, J. H.; Bando, Y.; Hu, J. Q.; Golberg, D. *Inorg. Chem.* **2004**, *43*, 2462.
(17) Zhou, J.; Gong, L.; Deng, S. Z.; Chen, J.; She, J. C.; Xu, N. S.; Yang, R.; Wang, Z. L. *Appl. Phys. Lett.* **2005**, *87*, 223108.
(18) Zhou, J.; Ding, Y.; Deng, S. Z.; Xu, N. S.; Wang, Z. L. *Adv. Mater.* **2005**, *17*, 2107.
(19) Zhu, Y. Q.; Hu, W. B.; Hsu, W. K.; Terrones, M.; Grobert, N.; Hare, J. P.; Kroto, H. W.; Walton, D. R. M.; Terrones, H. *Chem. Phys. Lett.* **1999**, *309*, 327.
(20) York, A. P. E.; Sloan, J.; Green, M. L. H. *Chem. Commun.* **1999**, 269.
(21) Hu, W. B.; Zhu, Y. Q.; Hsu, W. K.; Chang, B. H.; Terrones, M.; Grobert, N.; Terrones, H.; Hare, J. P.; Kroto, H. W.; Walton, D. R. M. *Appl. Phys. A* **2000**, *70*, 231.
(22) Gu, G.; Zheng, B.; Han, W. Q.; Roth, S.; Liu, J. *Nano Lett.* **2002**, *2*, 849.
(23) Hudson, M. J.; Peckett, J. W.; Harris, P. J. F. *J. Mater. Chem.* **2003**, *13*, 445.
(24) Li, X. L.; Liu, J. F.; Li, Y. D. *Inorg. Chem.* **2003**, *42*, 921.
(25) Jin, Y. F.; Zhu, Y. Q.; Whitby, R. L. D.; Yao, N.; Ma, R. Z.; Watts, P. C. P.; Kroto, H. W.; Walton, D. R. M. *J. Phys. Chem. B* **2004**, *108*, 15572.
(26) Hong, K. Q.; Xie, M. H.; Wu, H. S. *Nanotechnology* **2006**, *17*, 4830.
(27) Jeon, S.; Yong, K. *Nanotechnology* **2007**, *18*, 245602.
(28) Hong, K.; Xie, M. H.; Hu, R.; Wu, H. S. *Appl. Phys. Lett.* **2007**, *90*, 173121.
(29) She, J. C.; An, S.; Deng, S. Z.; Chen, J.; Xiao, Z. M.; Zhou, J.; Xu, N. S. *Appl. Phys. Lett.* **2007**, *90*, 073103.
(30) Li, Y. B.; Bando, Y.; Golberg, D. *Adv. Mater.* **2003**, *15*, 1294.
(31) Lou, X. W.; Zeng, H. C. *Inorg. Chem.* **2003**, *42*, 6169.
(32) Chen, D.; Ye, J. H. *Adv. Funct. Mater.* **2008**, in press, doi: 10.1002/adfm.200701468.
(33) Gu, G.; Zheng, B.; Han, W. Q.; Roth, S.; Liu, J. *Nano Lett.* **2002**, *2*, 849.
(34) Shen, G. Z.; Bando, Y.; Golberg, D. *Cryst. Growth Design* **2007**, *7*, 35.
(35) Shen, G. Z.; Bando, Y.; Ye, C. H.; Liu, B. D.; Golberg, D. *Nanotechnology* **2006**, *17*, 3468.
(36) Zhan, J. H.; Bando, Y.; Hu, J. Q.; Xu, F. F.; Golberg, D. *Small* **2005**, *1*, 883.
(37) Banhart, F. *Rep. Prog. Phys.* **1999**, *62*, 1181.